Graphical abstract

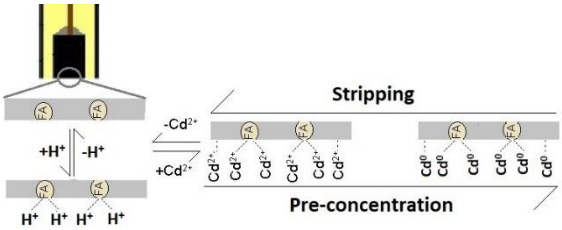

Development of coal fly ash modified graphite-polyurethane composite electrodes for the determination of Cd(II) in batteries and water

Caio R. de Barros[a], Priscila Cervini[a], Rafael M. Buoro[a],

Elizabet M. van der Merwe[b] and Éder T. G. Cavalheiro[a*]

[a]Instituto de Química de São Carlos, Universidade de São Paulo, Av. Trabalhador São-carlense, 400, CEP 13566-590, São Carlos, SP. Brazil

[b]Chemistry Department, University of Pretoria, Lynnwood Road, Pretoria, 0002, South Africa

*Corresponding author: cavalheiro@iqsc.usp.br

Abstract

Coal fly ash (FA), an aluminium silicate by-product and environmental pollutant which is generated during the combustion of coal in coal-fired power stations, was used as electrode modifier for the determination of Cd(II) in aqueous solutions. In this work, graphite/polyurethane-based composites containing different amounts of FA were prepared and characterized by SEM, EDX and TGA/DTG. The graphite/polyurethane composite electrodes (GPUE), with and without FA modifier, were evaluated with regard to their performance as voltammetric electrodes in the determination of metallic cations, using Cd(II) as a probe. After optimizing solution and instrumental parameters affecting the voltammetric peak current, a differential pulse anode stripping voltammetry (DPASV) procedure was developed for GPUE modified with 5% FA (*m/m*), resulting in a linear response for Cd(II) in the range 2.0 x 10^{-7} to 1.0 x 10^{-6} mol L^{-1} with a detection limit (LOD) of 6.6 x 10^{-8} mol L^{-1}. Cd(II) was added to natural water samples and determined in concentrations at 10^{-7} mol L^{-1} level, with a mean recovery of 99%. It was also extracted from exhausted rechargeable Ni-Cd batteries and diluted to ca. 0.2 µmol L^{-1} and determined with the same electrode, with recoveries of 98.7% when compared to FAAS. These results serve as a proof of concept that FA is a useful electrode modifier.

Keywords: Composite electrode, Differential pulse anodic stripping voltammetry, Metallic cation determination, Coal fly ash

Introduction

Coal fly ash (FA) is a by-product generated during the combustion of pulverized coal in thermoelectric power plants. It originates from the lighter particles that rise with the flue gases during combustion and is collected using electrostatic precipitators or bag filtering systems (van der Merwe et al. 2014). As a residue with high pollutant potential, with millions of tonnes being produced annually (Ge, Yoon, and Choi 2018), alternatives for the use of FA have been sought as a way to remove it from the environment. The most common include its incorporation into cement, concrete and bricks, i.e., in civil construction (Wu, Chi, Huang 2014; Zhang et al. 2020; Woszuk, Bandura, and Franus 2019). Other uses include improvement of soils for agriculture (Yao et al. 2015), synthesis of zeolites (Ameh et al. 2016) and geopolymers (Blissett and Rowson 2012) and the extraction of valuable elements such as aluminium (van der Merwe 2017).

FA particles present interesting physical features such as a spherical morphology, relatively low particle size distribution, smooth surface topography and high thermal stability, leading to a pursuit of highly valuable applications e.g., its potential application as polymer filler (van der Merwe, Mathebula, and Prinsloo 2014), as an absorbent for air and water pollutants (Ge, Yoon, and Choi 2018) and extraction of valuable metals (Vilakazi et al. 2022). The only reference found in literature regarding the electrochemical application of FA relates to the use of FA as binder in supercapacitor electrodes, based on activated carbon, for the determination of specific capacitance (Martinović et al. 2017). According to our knowledge, the use of FA as electrode modifier intended for electroanalysis, as done with other silicates (Cesarino et al. 2007), has not been reported.

The graphite-polyurethane composite electrode (GPUE) used in this work offers advantages such as high hydrophobicity, resistance to non-aqueous solvents and a wide useful potential window in both acidic and basic media. In addition, it is easy to incorporate different types of modifiers since it is prepared from a liquid polymer (Mattioli, Cervini, and Cavalheiro 2020). Our group has published several papers using this electrode, without (Mendes, Calero-Neto, and Cavalheiro 2002; Cervini and Cavalheiro 2008; Calixto, Cervini, and Cavalheiro 2012) and with modification (Santos and Cavalheiro 2014; Baccarin, Cervini, and Cavalheiro 2018), but this is the first attempt of using FA as a modifier.

In industry, cadmium is used in conjunction with nickel in rechargeable batteries, in pigments, deposited on various metals due to its resistance to corrosion, in alloys with other metals, and as impurity in the extraction of zinc (Pacer, Ellis, and Peng 1999). There are many papers describing the use of different electrodes for the determination of Cd(II) in water (Hu et al. 2019; Hassanpoor and Rouhi 2021), the simultaneous determination of Cd(II) and Pb(II) in water (Guenang et al. 2020; Oularbi, Turmine, and el Rhazi 2019; van Staden and Arnold Tatu 2019), herbal food supplements (Palisoa and Vitto 2019), decorative materials (Hou et al. 2020), hair (Manihandan and Narayanan 2019), bivalve molluscs (Pizarro et al. 2019) and paint (Cui and Li 2019), among others. Other examples describe the simultaneous determination of Cd(II), Pb(II) and Cu(II) using modified glassy carbon in water (Hassan, Elhaddad, and AbdelAzzem 2019) and parts of cigarettes (Walcarius 1999). Only one reference was found concerning the voltammetric determination of Cd in batteries (Aglan, Hamed and Saleh 2019). In that paper, Aglan et al. (2019) used a carbon paste electrode modified with lanthanum tungstate ion exchanger to determine Cd, reaching a limit of detection of 8.0×10^{-8} mol L^{-1}.

It is well known that silicas can be used to improve electrode sensitivity in electroanalytical procedures by preconcentrating cationic species (Walcarius 1999). Our group successfully used modified amorphous SBA-15 silica as a graphite polyurethane composite electrode modifier in the determination of several cationic species in water and ethanol media (Cesarino et al. 2007; Mendes, Claro-Neto, and Cavalheiro 2002). Considering that FA consists mostly of aluminium silicates, this work proposes the use of this material to act as electrode modifier by pre-concentration of cationic species.

The main objective of this work was to demonstrate the possibility of using FA as an electrode modifier and its features for metal ion analysis. Therefore, it was necessary prepare, characterize and apply a graphite-polyurethane composite electrode modified with FA (GPUE-FA) in the determination of a metallic cation, as a “proof of concept” of its viability. In this case Cd(II) in Ni-Cd rechargeable batteries and natural water samples were used as a probe. Up to our knowledge this is the first attempt of applying FA as an electrode modifier as alternative for the reuse of this relevant environmental pollutant. Due to its remarkable environmental importance and toxicity, in addition to its wide industrial use and well-known voltammetric behaviour, Cd (II) was chosen as the electroanalytical probe.

Experimental

Reagents and materials

A commercial-grade FA sample was obtained from Ash Resources, South Africa. This FA sample is marketed as an ultrafine spherical alumina-silicate polymer filler with a low carbon content and is specified to have a mean particle size of 4.5 μm, with more than 99% of the volume distribution of its particles having a diameter smaller than 25 μm. Detailed bulk and surface characterization of this sample was reported elsewhere (van der Merwe et al. 2014). Briefly, it consisted of an amorphous alumina-silicate glass phase (62.1%), which co-existed with two primary crystalline phases, mullite ($Al_6Si_2O_{13}$; 31.8%) and quartz (SiO_2; 6.1%). XRF analysis indicated the presence of six major chemical constituents (SiO_2, 49.3%; Al_2O_3, 34.0%; Fe_2O_3, 5.8%; CaO, 5.1%; TiO_2, 2.0% and MgO, 1.0%) and a low loss on ignition (LOI <0.6%).

All chemicals used in this work were of analytical grade and was used without further purification. Graphite powder (particle size < 20 μm), methylene diphenyl isocyanate (MDI) and castor oil (both from Univar, Brazil).

All solutions were prepared using water treated in a reverse osmosis system (Gehaka OS10 LZ, Brazil) and then purified in a Barnstead D13321 EasyPure RoDi® system (Thermo Scientific), with resistivity ≥ 18 MΩ cm^{-1}. A 1.0 x 10^{-3} mol L^{-1} Cd(II) standard stock solution was prepared from a 1000 mg L^{-1} standard solution (SpecSol®). Working solutions were prepared daily by appropriate dilutions of the Cd(II) stock solution in 0.10 mol L^{-1} KCl at different pHs, adjusted with HCl (Mattioli, Cervini, and Cavalheiro 2020).

Instrumentation

Electrochemical data were obtained using an Autolab PGSTAT 204 potentiostat/galvanostat, equipped with a FRA32 module for Electrochemical Impedance Spectroscopy (EIS) measurements, controlled by NOVA software (version 2.1.1) all from Metrohm.

Electrochemical measurements were performed in a three-electrode cell. The counter electrode was a platinum wire (1.0 cm length and diameter of 1.0 mm), and a saturated calomel

electrode (SCE, Hg/ Hg_2Cl_2) was used as the reference electrode. GPUE and GPUE-FA were used as the working electrodes, both with a geometric area of 0.070 cm^2 (diameter of 3.0 mm).

A Zeiss model LEO (440kV), with 63 kV resolution was used to collect SEM-EDX data at room temperature. SEM images were collected to evaluate the mean size and distribution of FA on the electrode surface of GPUE-FA while EDX was performed to evaluate the compositions of FA and GPUE-FA, respectively. The samples were sputter-coated with gold in a Bal-Tec Med 020 high vacuum coating system.

Thermogravimetric curves (TGA/DTG) were obtained in an SDT-Q600 thermogravimetric modulus controlled by a Universal Analysis software (both from TA Instruments), using sample masses of 6.5 ± 0.1 mg in open α-alumina sample holders at atmospheric pressure. The heating rate was 10 °C min^{-1} under N_2 until 600 °C and then under dynamic air atmosphere until 1000 °C. The gas flow was 100 mL min^{-1} in both cases.

Flame Atomic Absorption Spectrometric (FAAS) analysis were performed in a PINAACLE 900T (Perkin Elmer) to determine the Cd(II) concentration in the water and battery samples, to compare the results with those obtained using the GPUE-FA electrode. The concentrations of concomitants present in the natural water samples were also estimated by FAAS.

Wettability of the electrodes were evaluated by measuring the Contact Angles in a C201 optical tensiometer (Attension) equipped with a Navitar digital camera (Navitar) and controlled by One Attension software (Attension). A drop of water was added to the surface of the composites and 50 optical scans were performed to verify the contact angle formed between the solution and the surface. The left and right contact angles of water with the composite surfaces were determined and the average was calculated.

Preparation of the graphite-polyurethane composite electrode (GPUE) and the graphite-polyurethane composite electrode modified with FA (GPUE-FA)

Preparation and best composition of the unmodified graphite-polyurethane composite (GPU) and its electrode was previously established by Mendes et al. (2002). Briefly, a 2.85:1.1:0.8 graphite, MDI and castor oil mixture was homogenized for 5 min in a glass mortar,

pressed in a manual press, extruded as 3.0 mm diameter rods, and allowed to cure for 24 h at room temperature, after which the rods were cut into 1.0 cm sections. The rods were then connected to copper wires using a Conductive Silver Epoxy kit (Electron Microscopy Sciences). After 24 h, the composite/copper wire assembly was inserted into a glass tube (6.0 mm i.d., 8.5 cm length), sealed with SQ 3024 epoxy resin (Silaex) and allowed to cure for 24 h. Mechanical polishing with 2000 grit sandpaper was performed in an APL 02 motorized polisher (Arotec) to remove excess of epoxy resin from the surface and expose the composite. The electrode was sonicated in isopropanol for 5 min and then in water for additional 5 min before each working day. The GPU composites modified with FA (GPU-FA) were prepared using the compositions described in Table 1. The same preparation, assembly and activation process used for GPUE was adopted for the FA modified electrodes (GPUE-FA).

Table 1

Procedures

Solution and instrumental parameters affecting the voltammetric peak current were optimised for GPUE-FA 5% at room temperature, before a differential pulse anode stripping voltammetry (DPASV) procedure was developed. Factors that could potentially influence the analytical signal were the following: modifier loading, electrolyte medium, pH, pulse amplitude (A), scan rate (v), accumulation time (t_{acc}) and accumulation potential (E_{acc}).

The best modifier loading (2.5%, 5% and 10% FA, *m/m*) was determined by comparing the cyclic voltammetric curves obtained from using GPUE and GPUE-FA in solutions of 1.0×10^{-3} mol L^{-1} potassium ferricyanide and 1.0×10^{-4} mol L^{-1} $CdCl_2$ in 0.10 mol L^{-1} KCl at pH 3, respectively.

EIS measurements were performed using 5.0×10^{-3} mol L^{-1} potassium ferricyanide in 1.0 mol L^{-1} KCl at pH 3 by varying the frequency from 50000 to 1 Hz and applying 0.22 V (*vs*. SCE).

Solutions of 1.0×10^{-5} mol L^{-1} Cd(II) in 0.10 mol L^{-1} KCl, LiCl or dibasic potassium phosphate at pH 3, as established previously (Mendes, Claro-Neto, and Cavalheiro 2002) were evaluated as electrolyte mediums for GPUE-FA 5%, using cyclic voltammetry at a scan rate of 50 mV s^{-1}.

The effect of pH (2.0, 3.0, 4.0 and 5.0) on the voltammetric response of GPUE-FA 5% was evaluated by differential pulse voltammetry (DPV), using a solution of 1.0 x 10^{-5} mol L^{-1} Cd(II) in 0.1 mol L^{-1} KCl at pH 3 between -1.0 and -0.4 V (*vs*. SCE). Optimization of the differential pulse anodic stripping voltammetry (DPASV) parameters was performed according to a 2^n factorial planning, for n = 2 (pulse amplitude, a, and scan rate, v), resulting in four measurements, in which a = 25 and 50 mV, and v = 5 and 10 mV s^{-1}. This study was performed using GPUE-FA 5%, with 1.0 x 10^{-5} mol L^{-1} Cd(II) in 0.10 mol L^{-1} KCl at pH 3.0. The best accumulation time (15, 30, 60, 90, 120, 150, 180, 210, 240, 270 and 300s) and accumulation potential (-0.80, -0.85, -0.90, -0.95 and -1.0 V *vs*. SCE) were determined using DPASV under similar conditions.

Analytical curves were obtained in triplicate for Cd(II) solutions with concentrations ranging between 1.0 x 10^{-7} and 1.0 x 10^{-6} mol L^{-1}, using GPUE and GPUE-FA 5% under the optimized DPASV conditions (KCl 0.1 mol L^{-1}, pH = 3, t_{acc} = 3 min, a = 50 mV, v = 10 mV s^{-1}, E_{acc} = -1.0 V (*vs*. SCE).

For the determination of Cd(II) in batteries, an exhausted Ni-Cd battery was unassembled and the different layers were carefully separated, according to the STA-eletrônica user's manual (Sistemas e Tecnologia Aplicada 2023). The anode, made of $Cd(OH)_2$, and was chosen for analysis. The anode material was separated, and 1.0 g weighed (with precision of ± 0.1 mg) and kept under reflux in 0.5 mol L^{-1} sulfuric acid for 30 minutes, according to Freitas and Rosalém (2015). After the dissolution of $Cd(OH)_2$, the suspension was hot filtered on a sintered glass filter under reduced pressure.

According to the STA-eletrônica user's manual (Sistemas e Tecnologia Aplicada 2023), the concentration of Cd(II)in the leaching solution should be ca. 2.0 x 10^{-2} mol L^{-1}. After diluting this stock solution to 2.0 x 10^{-4} mol L^{-1}, 10 µL were added to the cell containing 20.0 mL of a 0.10 mol L^{-1} KCl solution at pH 3, resulting in a 2.0 x 10^{-7} mol L^{-1} Cd^{2+} estimated working concentration. After that, three 10.0 µL standard additions from the 1000 mg L^{-1} standard Cd(II)stock solution were performed in order to reach a 2.0 x 10^{-7} mol L^{-1} Cd(II) and DPASV measurements were performed in triplicate at GPUE-FA 5% after each standard addition.

Bottled mineral water was purchased at a local market. A tap water sample was collected straight from the public supply at USP Campus at São Carlos/SP, Brazil, while the artesian well water sample was collected from the Production and Distribution Center of the public water supply company of São Carlos at 22.021(W); 47.887(S). Tap and artesian well waters were collected in polypropylene vessels and kept in a refrigerator until use. All the water samples were spiked with a Cd(II) standard solution to be 2.0 x 10^{-7} mol L^{-1} and a suitable amount of solid KCl was dissolved in each to reach a KCl concentration of 0.10 mol L^{-1}, while the pH was adjusted to 3.0 with HCl. Finally, 20.0 mL aliquots were inserted in the voltammetric cell and DPASV voltammograms were taken in triplicate, under the optimized parameters. After that, three standard additions from the 1000 mg L^{-1} standard Cd(II)stock solution were performed in order to reach 2.0; 4.0 and 6.0 x 10^{-7} mol L^{-1} Cd(II) respectively and the voltammograms were recorded under the optimised conditions for each one. The procedure was repeated in triplicate for each water sample.

Results and discussion

Characterization of the GPU-FA composite

SEM images of the fractured and polished surfaces of the GPU-FA 5% composite were obtained at different magnifications (Figure 1). FA particles with particle sizes ranging between 2 and 10 µm were widely distributed throughout the composite, without any evidence of agglomeration (Figures 1 c, d). The two images in Figures 1b and 1d show the same frame, presented with different contrasts to better observe the details of insertion of the FA particles into the composite matrix. Figure 1d indicated tight bonding between FA and the composite matrix. Spherical shaped cavities could also be observed (Figure 1c), probably as a result of FA spheres being removed during surface polishing. The images of the fractured surfaces (Figures 1 a, b) showed that the FA particles were inserted in the composite, suggesting that they were embedded in the bulk of the composite matrix.

EDX analysis of GPU-FA 5% performed on the areas presented in Figure 1 and focused on the GPU matrix, i.e., the area outside the FA particles, presented 98.5% carbon and traces of iron, potassium and calcium impurities as well as small amounts of silicon and

aluminium, probably from the FA modifier (Table S1, Supplementary File). This result was anticipated, since most of the composite consisted of graphite and polyurethane, which mainly consists of carbon. Gold from the sputter-coating process could also be detected. When focusing on the FA spheres of the composite surface (Table S1, Supplementary File), several other elements were detected. O, Al and Si were the major elements, while Mg, K, Ca and Fe were observed in smaller quantities. These observations agree with the previously reported composition of FA (van der Merwe et al. 2014).

Figure 1

The wettability of the composites was evaluated by contact angle measurements. The contact angle for the unmodified GPU composite was (77.5 ± 0.4) ^{o}, while that of GPU-FA 5% composite was (84.8 ± 0.2) ^{o}, suggesting that both composites presented a certain degree of wettability. The small difference in the results obtained for GPU and GPU-FA 5% was attributed to the fact that, due to the manual nature of the polishing process, neither electrode was perfectly flat. The reason for the relative hydrophobicity in both cases was ascribed to the hydrophobic nature of polyurethane, which comprises almost 40% of the composite's mass.

Thermogravimetric curves were obtained for the GPU-FA composites to confirm that the modifier loadings were indeed 2.5, 5 and 10% (*m/m*). The TGA/DTG data obtained for the GPU and GPU-FA composites is summarized in Table S2 (Supplementary File). The FA modifier consisted of inorganic oxides (mainly silicon and aluminum) and had a loss on ignition below 0.6%, indicating that the sample contained a very low percentage of moisture, sulfur, unburned carbon, carbonates, and hydroxides (van der Merwe et al. 2014). Thermal treatment of the FA sample will therefore not contribute substantially to mass loss events occurring up to 900 °C, thus the observed mass loss events were ascribed to the decomposition of polyurethane and the combustion of graphite (Table S2). TGA/DTG analysis of the unmodified GPU composite resulted in a 0.53% residue at 900 °C. This amount was subtracted from the residues generated by the GPU-FA composites to obtain the amount of net residue, which was taken as the percentage of FA modifier in the GPU-FA composites. TGA/DTG analysis confirmed that the actual loadings of FA modifier in the GPU-FA composites compared well to the expected values (Table S2).

Determining the best modifier loading

The best modifier loading for the composite electrodes, GPUE and GPUE-FA, was evaluated using cyclic voltammetry and a 1.0 x 10^{-3} mol L^{-1} potassium ferricyanide solution in 0.10 mol L^{-1} KCl at pH 3 as a probe (Figure 2a). The lowest current intensities were observed at GPUE and GPUE-FA 10%, while at GPUE-FA 2.5% and GPUE-FA 5% the current intensities were almost the same, and 11% higher than the unmodified electrode. The explanation for this observation is two-fold. FA is a non-conductive material, while graphite is often used as electrically conductive filler in composite electrodes (Mendes, Claro-Neto, and Cavalheiro 2002). When conductive graphite active sites are replaced by non-conductive FA particles on the electrode surface, the electrochemical response of the composite is reduced. On the other hand, FA can interact with the analyte cations in solution, pre-concentrating them on the electrode surface, which in turn increases the electrochemical response of the device. Incorporation of 2.5% and 5% *(m/m)* FA modifier in the composite increased the voltammetric response of GPUE, indicating that the pre-concentration effect is more significant than the substitution of conductive graphite on the electrode surface when modifier loadings up to 5% *(m/m)* are used. However, at higher FA loadings (*c.a*. 10% (*m/m*)) the interaction with the metallic species is less significant than the occupation of the conductive graphite sites, resulting in a decreased current (Martinović et al. 2017; Mattioli, Cervini, and Cavalheiro 2020).

Figure 2

The same evaluation was performed for a 1.0 x 10^{-5} mol L^{-1} Cd(II) solution, using GPUE, GPUE-FA 2.5% and GPUE-FA 5%. Better results regarding shape and an increase of 23% in current intensity were obtained for the Cd(II) peak around -0.78 V (*vs*. SCE) using GPUE-FA 5%, when compared with GPUE-FA 2.5%, therefore it was subsequently chosen for further studies (Figure 2b).

Electrochemical Impedance Spectroscopy (EIS)

EIS measurements were used to compare the equivalent circuits of GPUE and GPUE-FA 5% and to determine the influence of the modifier on the electrical response of the electrodes. The equivalent circuits proposed for GPUE and GPUE-FA 5%, and the EIS Nyquist

graphs which were obtained from the proposed equivalent circuits, are presented in Figure 3. Values of the equivalent circuit parameters obtained from the EIS spectra of GPUE and GPUE-FA 5% are summarized in Table S3 (Supplementary File).

Figure 3a shows the equivalent circuit proposed for GPUE, in which two Randles circuits are observed in parallel, one of them having a Gerischer impedance (G) which could indicate that there are two sites where the electrochemical reaction is occurring. Considering that GPUE is a porous electrode and that the Gerischer impedance can be used to model such type of electrodes, it is likely that the two reaction sites occur at the electrode surface and the interior of the pores. The Gerischer element can be interpreted as an equilibrium between the outer and the inner part of the pores. Once inside the pore, the probe can transfer charge simultaneously at two different sites, which is represented by the two parallel Randles circuits. The Randles circuit in series with the Gerischer element represents charge transfer at the inner part of the pore, while the other Randles circuit represents charge transfer at the electrode outer surface. This assumption can be made since both the R_1 resistance (91.8 Ω) and W_1 Warburg Impedance (0.82 x 10^{-3} Mho $s^{1/2}$) are greater than R_2 (27.1 Ω) and W_2 (0.29 x 10^{-3} Mho $s^{1/2}$), which corroborates the hypothesis. Lastly, χ^2 for this circuit was determined to be 5 x 10^{-4} when fitted against the Bode modulus, Bode Phase and Nyquist graph (Table S3 and Figure 3c).

Figure 3

In Figure 3b, the equivalent circuit proposed for GPUE-FA 5% presents only one resistance associated to charge transfer on the graphitic surface. However, there are two constant phase elements (CPE), one close to the uniformity of a capacitor, shown by its N of 0.62 which can be associated to the electric double layer formation on the graphitic surface and another much more non-uniform, with an N of 0.95, which can be associated to FA modification of GPUE. The roughness and porosity presented by the GPUE base electrode creates a deviation from linearity as the distance between the polarized surface and the ions at the outer plane of Helmholtz varies throughout the entire surface. The elevated capacitance observed at CPE_2 (N = 0.95) compared to that of CPE_1 (N = 0.62) sustains that hypothesis.

The fact that the GPUE-FA equivalent circuit does not present a Gerischer element can be explained by the fact that FA contains alumina acidic sites (Gafurov et al. 2015), which when

in its basic form will repel the anionic probe, preventing it to enter the pores. In addition, since FA is a non-conducting aluminium-silicate species, it does not appear in the equivalent circuit as a separated charge transfer resistance, but only contributes to the surface capacitance.

FA is a harder material than graphite and therefore the polishing procedure and the sandpaper used to polish the graphite did not affect the morphology of the FA particles. This may explain why the capacitive behaviour of FA is close to that of an ideal capacitor, indicating low surface roughness for the electrode. The equivalent circuit for GPUE-FA 5% showed a χ^2 of 4×10^{-4} when fitted to the Nyquist graph (Table S3 and Figure 3d), indicating that it is an accurate interpretation of the electrode/solution interface.

Analytical Evaluation

The effect of varying the supporting electrolyte on the voltammetric response of GPUE-FA 5% during the determination of Cd(II) was studied by cyclic voltammetry of 1.0×10^{-4} mol L^{-1} $CdCl_2$ in 0.10 mol L^{-1} solutions of LiCl, phosphate and KCl at pH 3 (Figure 4). A higher current intensity (35 µA) was observed at ca. -0.81 V (vs. SCE) for the oxidation of Cd(II) in the KCl solution. KCl was therefore chosen as supporting electrolyte in subsequent experiments.

Figure 4

Figure 5 presents the results for optimization of pH, pulse amplitude, scan rate, accumulation time and accumulation potential in the voltammetric response of GPUE-FA 5%, evaluated by DPV and DPASV of 1.0×10^{-4} mol L^{-1} $CdCl_2$ in 0.10 mol L^{-1} KCl. The analytical curve obtained for the determination of Cd(II) under the optimized conditions is also shown.

Figure 5

The effect of the hydrogen ion concentration of the medium on the voltammetric response was evaluated at different pH values (Figure 5a). The obtained differential pulse voltammograms presented increased current intensity (0.59 µA at *c a*. -0.87 V (*vs*. SCE)) and a better peak profile for DPV measurements performed at pH 3. These results suggest a competition between the active sites of FA that seem to be protonated at pH ≤ 2.0 and chloride

complexes that are present in relevant concentrations at pH ≥ 4.0 (Vanderzee and Dawson 1953; Zirino and Yamamoto 1972).

The pulse amplitude and scan rate were optimized by DPASV according to 2^n factorial experimental planning, discussed in the experimental section. Pulse amplitude of 50 mV and scan rate of 10 mV s^{-1} were chosen to present the best voltammetric profile and peak current intensity (Figure 5b). Optimization of the accumulation potential (Figure 5c) displayed lower peak currents at lower accumulation potentials, especially for measurements performed at -0.80 and -0.85 V (*vs.* SCE). The stripping voltammogram obtained after accumulation at -0.85 V (*vs*. SCE) presented a peak displacement towards a more positive potential and a shoulder at the same potential as the voltammogram obtained after accumulation at -0.80 V (*vs*. SCE). This is probably due to an over deposit of Cd° on a first Cd° layer or a deposition in two different sites e.g. on both graphite and FA contained in GPUE-FA 5%. The highest peak currents (measured at *c.a*. -0.8 V (*vs*. SCE)) were obtained after applying -0.95 and -1.0 V (*vs*. SCE) as accumulation potentials, for which single peaks were observed in both instances. An accumulation potential of -1.0 V (*vs*. SCE) was chosen for further experiments.

The accumulation time (t_{acc}) was evaluated between 30 and 300 seconds (Figure 5d). For t_{acc} more than 180 s, the peak current tended towards a constant value. Therefore, t_{acc} = 180 s was chosen for further studies once above this accumulation time we conclude that the current increase was not enough to justify the lowering in the analytical frequency.

Analytical curves (Figure 5f) were obtained using the optimized parameters for DPASV at GPUE-FA 5% (Figure 5e), using Cd(II)solutions with concentrations ranging from 1.0 x 10^{-7} to 1.0 x 10^{-6} mol L^{-1}. For comparison, the same set of experiments was performed using the unmodified GPUE, which presented a similar response, however with lower peak currents.

At the unmodified GPUE, a linear dynamic range between 4.00 x 10^{-7} and 1.00 x 10^{-6} mol L^{-1} was observed, with a limit of detection (LOD) of 1.49 x 10^{-7} mol L^{-1} and R = 0.9990, for n = 4. The LOD was calculated as three times the standard deviation of the blank, divided by the slope, according to Long and Winefordner (1983). At GPUE-FA 5% a linear range (Figure 5f) was obtained between 2.0 x 10^{-7} and 1.0 x 10^{-6} mol L^{-1}, with an LOD of 6.61 x 10^{-8} mol L^{-1} and R = 0.9989, for n = 5. This LOD was comparable to recent studies of other electrode

compositions (van der Merwe 2014; Hu 2019), but lower than that observed for some more expensive or non-usual materials (Hu et al. 2019; Hassanpoor and Rouhi 2021; Guenang et al. 2020; Oularbi, Turmine, and el Rhazi 2019; van Staden and Arnold Tatu 2019). However, GPUE-FA has the advantage of being composed of inexpensive and recycled materials, making it more financially and environmentally friendly. Above 1.0 x 10^{-6} mol L^{-1}, a deviation from the linear response at both GPUE and GPUE-FA was observed, probably due to the response of graphite active sites at the electrode surface with the increasing in Cd(II) concentration. Both the sensitivity and linear range obtained were higher for GPUE-FA 5% in comparison with GPUE.

Determination of Cd(II) in battery samples

Aliquots of the solutions containing Cd(II) extracted from the anodes of exhausted Cd-Ni batteries were added to the cell containing 0.1 mol L^{-1} KCl solution at pH 3 in order to obtain a working concentration of ca. 2.0 x 10^{-7} mol L^{-1}. After that, three additions of 2.0 x 10^{-7} mol L^{-1} Cd(II) from standard solution were performed, and DPASV voltammograms were registered in triplicate using GPUE-FA 5% under the optimized conditions. Table 2 presents the of Cd(II) concentration determined by triplicate DPASV measurements for three different extractions of Cd from the batteries in comparison to the concentration determined by atomic absorption spectrometry (FAAS). The results obtained with GPUE-FA 5% agreed with those from FAAS in the 95% confidence level according to the Student's t-test. When comparing the results from DPASV via the standard addition method, with those from FAAS, the relative error (E_r) was determined to be less than 1.5% for each individual extraction experiment. This result demonstrates the effectiveness of GPUE-FA 5% for the determination of Cd(II), and reveals that the concomitant ions in the samples do not interfere in the determination.

Table 2

Determination of Cd(II) in water samples

Water samples, collected from three natural sources (artesian well, tap water and non-sparkling mineral bottled water), were spiked with Cd(II) standard solutions until a Cd(II) concentration of 2.0 – 3.0 10^{-7} mol L^{-1} was reached. The spiked water samples containing 0.10 mol L^{-1} KCl solution at pH 3 were added to a voltammetric cell. After that, three additions of 2.0 x 10^{-7} mol L^{-1} Cd(II) solution were performed and DPASV voltammograms were recorded in

triplicate using GPUE-FA 5%. The obtained results were compared with those from FAAS (Table 2).

The results obtained with GPUE-FA 5% agreed with those from FAAS in the 95% confidence level according to the t-test. When comparing the results from DPASV via the standard addition with those from FAAS, the relative error was less than 2% for each water sample tested. The effectiveness of GPUE-FA 5% for the determination of Cd(II) in water samples was therefore confirmed. These results are particularly noteworthy since each water sample contained different amounts and types of minerals due to their different origins. Furthermore, the initial Cd(II) concentrations of the water samples varied, showing the ability of the GPUE-FA 5% electrode to determine Cd(II) concentrations in different parts of the linear range.

The concentration of concomitant cations in the natural water samples investigated in this study was determined by FAAS (Table S4, Supplementary file). The presence of mainly Li, Na, Ca, Mg, Fe and Zn cations, up to the levels in which they naturally occur, did not interfere with the DPASV determination of Cd(II) using GPUE-FA 5%.

Additionally, the long-lasting useful life of the GPUE-FA 5% electrode was demonstrated by the fact that only one electrode was used for all the voltammetric determinations presented in this paper. These determinations were performed over a period of 6 months.

Proposal for the action of FA in the pre-concentration of metal ions

Figure 6 proposes a scheme to explain the effect of FA embedded in the GPU composite matrix with relation to the pre-concentration of metallic cations, according to observations made in the current study.

Functional groups on the FA surface can be reversibly protonated in a sufficiently acidic medium. This statement is justified by the reduction of the Cd(II) voltammetric signal in a medium of pH < 3 (Figure 5a). Therefore, this parameter requires optimization for DPASV measurements. Following optimization of the pH (i.e., acidity), the FA will have deprotonated surface functional groups which are free to interact with the metallic cation, thereby promoting

pre-concentration of the cation on the FA surface. This effect will lead to increased sensitivity in the voltammetric signal of the FA modified electrode, when compared to that of the unmodified electrode.

At adequate potential, Cd^{2+} is reduced and accumulated in the device, being oxidized in the redissolution (or stripping) step. Since a voltammetric response was also observed for the unmodified electrode, it is inferred that the GPU matrix also allows Cd^{2+} deposition on its surface. However, the presence of FA with its surface functional groups, intensifies this process.

All the steps involved proved to be reversible, allowing for the electrode to be reused without the need for surface renewal between successive measurements. This model can be applied to other metallic cations, under optimized conditions of electrolytic medium, pH, accumulation time and accumulation potential.

Conclusions

This work demonstrated that FA can be incorporated to a graphite-polyurethane composite to prepare modified voltammetric electrodes for determination of metallic cations in natural waters, as demonstrated using Cd^{2+} as an electroanalytical probe.

The presence of FA in the composite matrix was demonstrated by SEM, EDX and TG/DTG. The FA modifier was firmly supported in the GPU composite and it was distributed throughout the bulk of the material.

Electrochemical tests demonstrated that FA improved the sensitivity of the voltammetric response to potassium ferricyanide. It has furthermore shown that pre-concentration of Cd(II) on the FA surface may facilitate reaching limits of detection at sub-µmol L^{-1} level, when DPASV is used as detection technique.

EIS analysis showed that the addition of FA to the GPU composite influenced its equivalent circuit, due to the FA modifier occupying the empty pores of the GPU composite in such a way as to repel the analyte, preventing it from entering the pores with subsequent accumulation of the analyte at the electrode surface.

Cd(II) was successfully determined by DPASV using the GPUE-FA 5% electrode in the anodes of exhausted rechargeable batteries and in natural water samples, following spiking with standard solutions of $CdCl_2$. The results for determination of Cd(II) by DPASV agreed well with FAAS data. The presence of naturally occurring concomitants in the water samples had no influence on the accuracy of Cd(II) determinations.

The GPUE-FA electrodes were easy to construct, can be built at low cost, presented easiness of surface renovation once the FA modifier was dispersed in the whole bulk and had a sensitivity on par with other electrodes. The proposed FA modified GPU electrodes therefore presented a viable option for the reuse of a by-product an important environmental waste which is generated during combustion of coal in coal-fired power stations.

Acknowledgments

The work was financially supported by the National Research Foundation of South Africa (NRF; Grant number 119223). Support from Brazilian agencies CAPES (CRB master fellowship), CNPq and FAPESP were also acknowledged.

References

Aglan, R. F., Hamed, M. M., Saleh, H. M. 2019. Selective and sensitive determination of Cd(II) ions in various samples using a novel modified carbon paste electrode. J Anal Sci Technol 10:7. doi:https://doi.org/10.1186/s40543-019-0166-4.

Ameh, A. E., Musyoka, N. M., Fatoba, O. O., Syrtsova, D. A., Teplyakov, V., Petrik, L. F. 2016. Synthesis of zeolite NaA membrane from fused fly ash extract. *Journal of Environmental Science and Health, Part A* 51:348–56. doi:https://doi.org/10.1080/10934529.2015.1109410.

Baccarin, M., Cervini, P., Cavalheiro, E. T. G.2018. Comparative performances of a bare graphite-polyurethane composite electrode unmodified and modified with graphene and carbon nanotubes in the electrochemical determination of escitalopram. *Talanta* 178:1024–32. doi:https://doi.org/10.1016/j.talanta.2017.08.094.

Blissett, R. S., Rowson, N. A. 2012. A review of the multi-component utilisation of coal fly ash. *Fuel* 97:1–23. doi:https://doi.org/10.1016/j.fuel.2012.03.024.

Calixto, C. M. F., Cervini, P., Cavalheiro, E. T. G. 2012. Determination of tetracycline in environmental water samples at a graphite-polyurethane composite electrode. *Journal of Brazillian Chemical Society* 23:938–43. doi:https://doi.org/10.1590/S0103-50532012000500020.

Cervini, P., Cavalheiro, E. T. G. 2008. Graphite-Polyurethane Composite Electrode as an Amperometric Flow Detector in the Determination of Atenolol. *Analytical Letters* 41:1867–77. doi:https://doi.org/10.1080/00032710802162152.

Cesarino, I., Marino, G., Matos, J. R., Cavalheiro, E. T. G. 2007. Using the organofunctionalised SBA-15 nanostructured silica as a carbon paste electrode modifier: determination of cadmium ions by differential anodic pulse stripping voltammetry. *Journal of Brazillian Chemical Society* 18:810–7. doi:https://doi.org/10.1590/S0103-50532007000400021.

Cui, H., Li, Q. 2019. Multi-walled Carbon Nanotubes Modified Screen-Printed Electrode Coated Bismuth Oxide Nanoparticle for Rapid Detection of Cd(II) and Pb(II). *International Journal of Electrochemical Science* 14:6154–67. doi:https://doi.org/10.20964/2019.07.15.

Freitas, M. B. J. G, Rosalém, S. F. 2005. Electrochemical recovery of cadmium from spent Ni–Cd batteries. *Journal of Power Sources* 139:366–70. doi:https://doi.org/10.1016/j.jpowsour.2004.06.074.

Gafurov, M. R., Mukhambetov, I. N., Yavkin, B. V., Mamin, G. V., Lamberov, A. A., Orlinskii, S. B. 2015. Quantitative Analysis of Lewis Acid Centers of γ-Alumina by Using EPR of the Adsorbed Anthraquinone as a Probe Molecule: Comparison with the Pyridine, Carbon Monoxide IR, and TPD of Ammonia. *The Journal of Physical Chemistry C* 119:27410–5. doi:https://doi.org/10.1021/acs.jpcc.5b09759.

Ge, J. C., Yoon, S. K., Choi, N. J. 2018. Application of Fly Ash as an adsorbent for removal of air and water pollutants. *Applied Sciences* 8 (7):1116. doi:https://doi.org/10.3390/app8071116.

Guenang, L. S., Dongmo, L. M., Jiokeng, S. L. Z., Kamdem, A. T., Doungmo, G., Tonlé, I. K., et al. 2020. Montmorillonite clay-modified disposable ink-jet-printed graphene electrode as a sensitive voltammetric sensor for the determination of cadmium(II) and lead(II). *SN Applied Sciences* 2:476. doi:https://doi.org/10.1007/s42452-020-2283-5.

Hassan, K. M., Elhaddad, G. M., AbdelAzzem, M. 2019. Voltammetric determination of cadmium(II), lead(II) and copper(II) with a glassy carbon electrode modified with silver nanoparticles deposited on poly(1,8-diaminonaphthalene). *Microchimica Acta* 186:440. doi:https://doi.org/10.1007/s00604-019-3552-0.

Hassanpoor, S., Rouhi, N. 2021. Electrochemical sensor for determination of trace amounts of cadmium (II) in environmental water samples based on MnO_2/RGO nanocomposite. International Journal of Environmental Analytical Chemistry 101:513–32. doi:https://doi.org/10.1080/03067319.2019.1669582.

Hou, X., Xiong, B., Wang, Y., Wang, L., Wang, H. 2020. Determination of Trace Lead and Cadmium in Decorative Material Using Disposable Screen-Printed Electrode Electrically Modified with Reduced Graphene Oxide/L-Cysteine/Bi-Film. *Sensors* 20:1322. doi:https://doi.org/10.3390/s20051322.

Hu, S., Guowei, G., Ye, L., Jingfang, H., Yu, S., Xiaoping, Z. 2019. An Electrochemical Sensor Based on ion Imprinted PPy/rGO Composite for Cd(II) Determination in Water. *International of Journal Electrochemical Science* 14:11714–30. doi:https://doi.org/10.20964/2019.11.56.

Lisboa, T. P., de Faria, L. V., Matos, M. A. C., Matos, R. C., de Sousa, R. A. 2019. Simultaneous determination of cadmium, lead, and copper in the constituent parts of the illegal cigarettes by Square Wave Anodic Stripping Voltammetry. *Microchemical Journal* 150:104183. doi: https://doi.org/10.1016/j.microc.2019.104183.

Long, G. L., Winefordner, J. D. 1983. Limit of detection. A closer look at the IUPAC definition. *Analytical Chemistry* 55:712A-724A. doi:https://doi.org/10.1021/ac00258a001.

Manikandan, R., Narayanan, S. S. 2019. Simultaneous anodic stripping voltammetric determination of Pb(II) and Cd(II) using poly methyl thymol blue film–modified electrode. Ionics (Kiel) 25:6083–92. doi:https://doi.org/10.1007/s11581-019-03143-w.

Martinović, S., Vlahović, M., Ponomaryova, E., Ryzhkov, I. V., Jovanović, M., Bušatlić, I., Volkov, H. T., Stević, Z. 2017. Electrochemical Behavior of Supercapacitor Electrodes Based on Activated Carbon and Fly Ash. *International Journal Electrochemical Science* 12:7287–99. doi:https://doi.org/10.20964/2017.08.63.

Mattioli, I. A., Cervini, P., Cavalheiro, E. T. G. Screen-printed disposable electrodes using graphite-polyurethane composites modified with magnetite and chitosan-coated magnetite nanoparticles for voltammetric epinephrine sensing: a comparative study. *Microchimica Acta* 187 (318). doi:https://doi.org/10.1007/s00604-020-04259-x.

Mendes, R., Claro-Neto, S., Cavalheiro, E. T. G. 2002. Evaluation of a new rigid carbon–castor oil polyurethane composite as an electrode material. *Talanta* 57:909–17. doi:https://doi.org/10.1016/S0039-9140(02)00122-4.

Oularbi, L., Turmine, M., el Rhazi, M. 2019. Preparation of novel nanocomposite consisting of bismuth particles, polypyrrole and multi-walled carbon nanotubes for simultaneous voltammetric determination of cadmium(II) and lead(II). *Synthetic Metals* 253:1–8. doi:https://doi.org/10.1016/j.synthmet.2019.04.011.

Pacer, R., Ellis, C. K. S., Peng, R. 1999. Determination of cadmium in sewage sludge by differential pulse anodic stripping voltammetry. *Talanta* 49:725–33. doi:https://doi.org/10.1016/S0039-9140(99)00058-2.

Palisoc, S., Vitto, R. I. M., Natividad, M. 2019. Determination of Heavy Metals in Herbal Food Supplements using Bismuth/Multi-walled Carbon Nanotubes/Nafion modified Graphite Electrodes sourced from Waste Batteries. *Scientific Reports* 9: 18491. doi:https://doi.org/10.1038/s41598-019-54589-x.

Pizarro, J., Segura, R., Tapia, D., Bollo, S., Sierra-Rosales, P. 2019. Electroanalytical Determination of Cd(II) and Pb(II) in Bivalve Mollusks using Electrochemically Reduced Graphene Oxide-based Electrode. *Electroanalysis* 31:2199–205. doi:https://doi.org/10.1002/elan.201900061.

Santos, S. X. dos, Cavalheiro, E. T. G. 2014. Using of a Graphite-Polyurethane Composite Electrode Modified with a Schiff Base as a Bio-Inspired Sensor in the Dopamine Determination. *Journal of Brazillian Chemical Society* 25 (6):1071-77. doi:https://doi.org/10.5935/0103-5053.20140080.

Sistemas e Tecnologia Aplicada. www.sta-eletronica.com.br. 2023. Manual das Baterias Recarregáveis, Pilhas e Carregadores. n.d.

van der Merwe, E. M., Prinsloo, L. C., Mathebula, C. L., Swart, H. C, Coetsee, E., Doucet, F. J. 2014. Surface and bulk characterization of an ultrafine South African coal fly ash with reference to polymer applications. *Applied Surface Science* 317:73–83. doi:https://doi.org/10.1016/j.apsusc.2014.08.080.

van der Merwe, E. M, Gray, C. L., Castleman, B. A., Mohamed, S., Kruger, R. A., Doucet, F. J. 2017. Ammonium sulphate and/or ammonium bisulphate as extracting agents for the recovery of aluminium from ultrafine coal fly ash. *Hydrometallurgy* 171:185–90. doi:https://doi.org/10.1016/j.hydromet.2017.05.015.

van der Merwe, E. M., Mathebula, C. L., Prinsloo, L.C. 2014. Characterization of the surface and physical properties of South African coal fly ash modified by sodium lauryl sulphate (SLS) for applications in PVC composites. *Powder Technology* 266:70–8. doi:https://doi.org/10.1016/j.powtec.2014.06.008.

Vanderzee, C. E., Dawson, H. J. 1953. The Stability Constants of Cadmium Chloride Complexes: Variation with Temperature and Ionic Strength [1]. *Journal of American Chemical Society* 75 (22):5659–63. doi:https://doi.org/10.1021/ja01118a056.

van Staden, J. F., Arnold Tatu, G-L. 2019. Modified graphite/graphene dot microsensors for the assay of trace amounts of lead and cadmium in water catchments areas using differential pulse anodic stripping voltammetry. *Revue Roumaine de Chimie* 64 (10):867–77. doi:https://doi.org/10.33224/rrch/2019.64.10.05.

Vilakazi, A.Q., Ndlovu, S., Chipise, L., Shemi, A. 2022. The Recycling of Coal Fly Ash: A Review on Sustainable Developments and Economic Considerations. *Sustainability* 14 (4):1958. doi:https://doi.org/10.3390/su14041958.

Walcarius, A. 1999. Analytical Applications of Silica-Modified Electrodes -A Comprehensive Review. *Electroanalysis* 10:1217–35. doi:https://doi.org/10.1002/(SICI)1521-4109(199812)10:18<1217::AID-ELAN1217>3.0.CO;2-X.

Woszuk A., Bandura, L., Franus, W. 2019. Fly ash as low cost and environmentally friendly filler and its effect on the properties of mix asphalt. *Journal of Cleaner Production* 235:493–502. doi:https://doi.org/10.1016/j.jclepro.2019.06.353.

Wu, T., Chi, M., Huang, R. 2014. Characteristics of CFBC fly ash and properties of cement-based composites with CFBC fly ash and coal-fired fly ash. *Construction and Building Materials* 66:172–80. doi:https://doi.org/10.1016/j.conbuildmat.2014.05.057.

Yao, Z. T., Ji, X. S., Sarker, P. K., Tang, J. H., Ge, L. Q., Xia, M. S., Xi, Y. Q. 2015. A comprehensive review on the applications of coal fly ash. *Earth-Science Reviews* 141:105–21. doi:https://doi.org/10.1016/j.earscirev.2014.11.016.

Zhang, P., Gao, Z., Wang, J., Guo, J., Hu, S., Ling, Y. 2020. Properties of fresh and hardened fly ash/slag based geopolymer concrete: A review. *Journal of Cleaner Production* 270:122389. doi:https://doi.org/10.1016/j.jclepro.2020.122389.

Zirino, A., Yamamoto, S. 1972. A pH-dependent model for the chemical speciation of copper, zinc, cadmium, and lead in seawater. *Limnology and Oceanography* 17 (5):661–71. doi:https://doi.org/10.4319/lo.1972.17.5.0661.

Table 1 Composition of the GPU-FA composites

Composite	Composition / (%, *m/m*)		
	Graphite	**PU**	**FA**
GPU	60.0	40.0	0
GPU-FA 2.5%	58.7_5	38.7_5	2.5
GPU-FA 5%	57.5	37.5	5.0
GPU-FA 10%	55.0	35.0	10.0

Table 2 Results of Cd content in battery extracts and spiked water samples using DPASV at GPUE-FA 5% and FAAS

Extraction	Sample	Concentration / mol L^{-1}		Recovery / %
		DPASV	FAAS[a]	
1st	**1**	2.76×10^{-7}		102.6
	2	2.62×10^{-7}	$(2.7 \pm 0.1) \times 10^{-7}$	97.0
	3	2.59×10^{-7}		95.9
	Mean[a]	$(2.66 \pm 0.05) \times 10^{-7}$		99 ± 4
	Relative error, E_r [b]	E_r = 1.5 %		
2nd	**1**	2.20×10^{-7}		95.6
	2	2.39×10^{-7}	$(2.3 \pm 0.2) \times 10^{-7}$	103.9
	3	2.26×10^{-7}		98.2
	Mean[a]	$(2.28 \pm 0.05) \times 10^{-7}$		99 ± 4
	Relative error[b]	E_r = 0.87 %		
3rd	**1**	2.03×10^{-7}		96.7
	2	2.16×10^{-7}	$(2.1 \pm 0.1) \times 10^{-7}$	102.8
	3	2.05×10^{-7}		97.6
	Mean[a]	$(2.08 \pm 0.04) \times 10^{-7}$		99 ± 3
	Relative error[b]	E_r = 0.95 %		
Artesian well water	**1**	3.02×10^{-7}		95.9
	2	3.19×10^{-7}	$(3.15 \pm 0.05) \times 10^{-7}$	101.3
	3	3.26×10^{-7}		103.5
	Mean[a]	$(3.16 \pm 0.07) \times 10^{-7}$		100 ± 4
	Relative error[b]	E_r = 0.32 %		
Tap water	**1**	2.42×10^{-7}		97.2
	2	2.60×10^{-7}	$(2.49 \pm 0.05) \times 10^{-7}$	104.4
	3	2.53×10^{-7}		101.6
	Mean[a]	$(2.52 \pm 0.05) \times 10^{-7}$		101 ± 4
	Relative error[b]	E_r = 1.2 %		
Mineral water	**1**	2.27×10^{-7}		103.2
	2	2.12×10^{-7}	$(2.2 \pm 0.2) \times 10^{-7}$	96.4
	3	2.10×10^{-7}		95.4
	Mean[a]	$(2.16 \pm 0.05) \times 10^{-7}$		98 ± 4
	Relative error[b]	E_r = 1.8 %		

[a] mean ± standard deviation; n = 3
[b] relative error: E_r = [DPASV – FAAS)/FAAS] * 100

Barros et al. Fig. 1

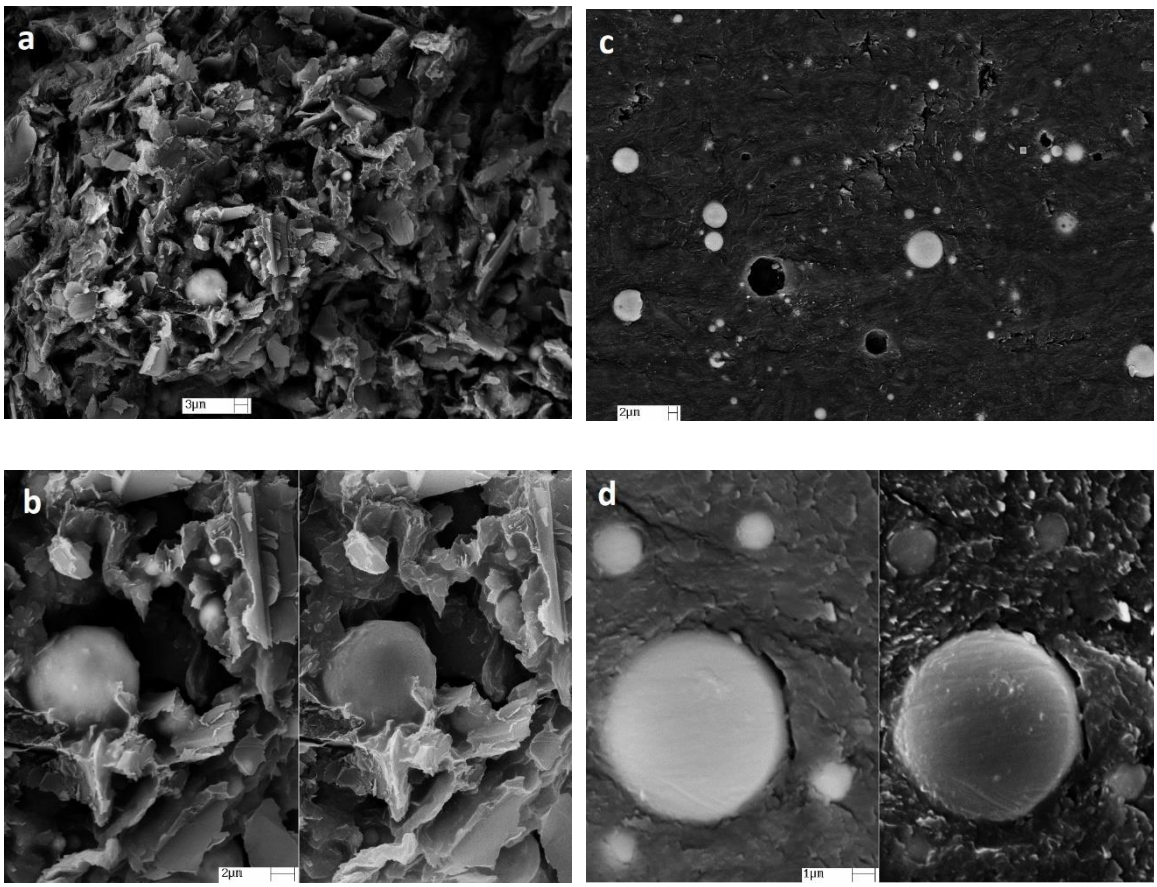

Fig. 1 SEM micrographs obtained for the fractured GPU-FA 5% composite at (a) 3 000X and (b) 8 000X magnifications and polished GPU-FA 5% at (c) 3 000X and (d) 15 000X magnifications. In images (b) and (d) the same frame is presented at different contrasts to better observe the details of insertion of the FA particle into the composite matrix.

Barros et al – Fig.2

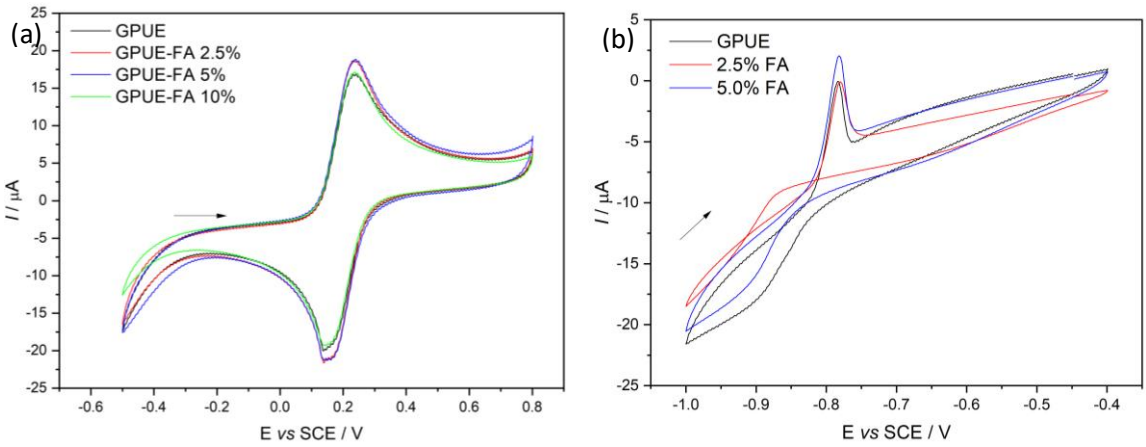

Fig. 2 Cyclic voltammograms using GPUE (without modifier) and GPUE-FA (2.5, 5.0, 10% (*m/m*) FA modifier) in solutions of (a) 1.0 x 10^{-3} mol L^{-1} potassium ferricyanide and (b) 1.0 x 10^{-4} $CdCl_2$, both in 0.10 mol L^{-1} KCl at pH = 3.0, v = 50 mV s^{-1}.

Barros et al – Fig. 3

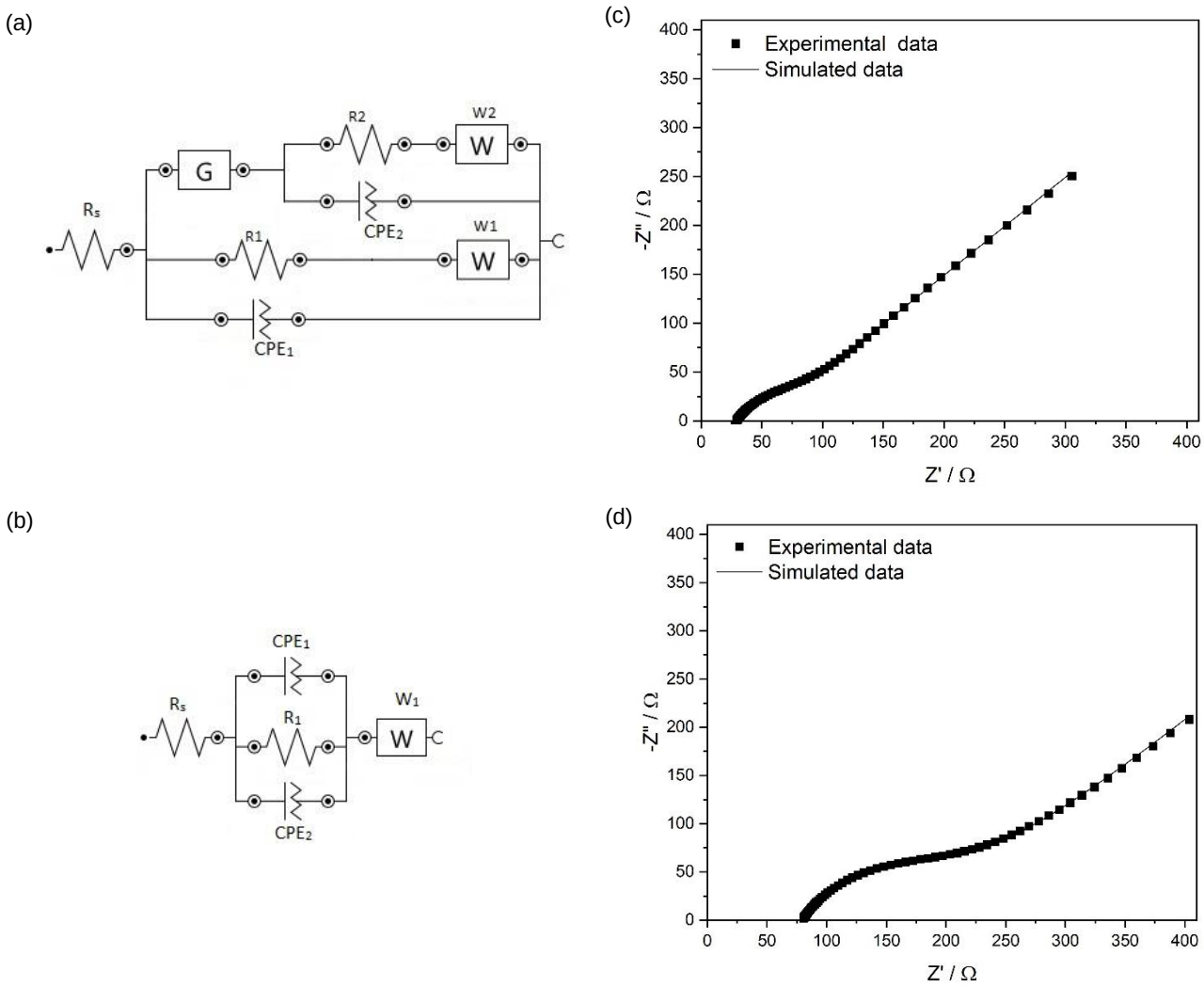

Fig. 3. Equivalent circuit proposed for (a) GPUE and (b) GPUE-FA 5% and EIS Nyquist graphs fitting experimental points (■) with simulated data (─) from the proposed equivalent circuits for (c) GPUE and (d) GPUE-FA 5%.

Barros et al. – Fig. 4

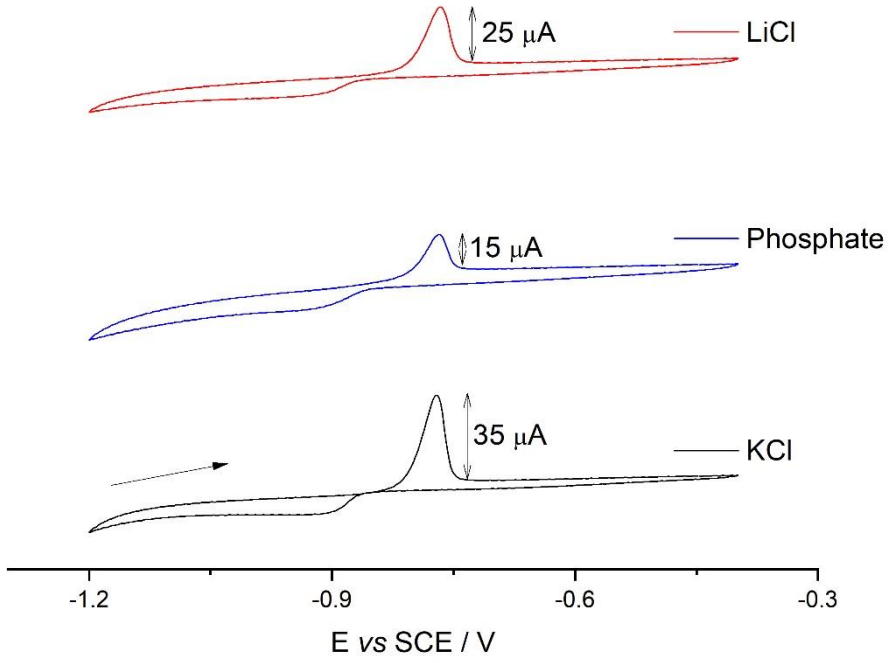

Fig. 4 – Cyclic voltammograms obtained at v = 50 mV s^{-1} for GPUE-FA 5% in the presence of 1.0 x 10^{-4} mol L^{-1} Cd(II) in 0.10 mol L^{-1} solutions of LiCl, phosphate and KCl at pH 3.

Barros et al. – Fig. 5

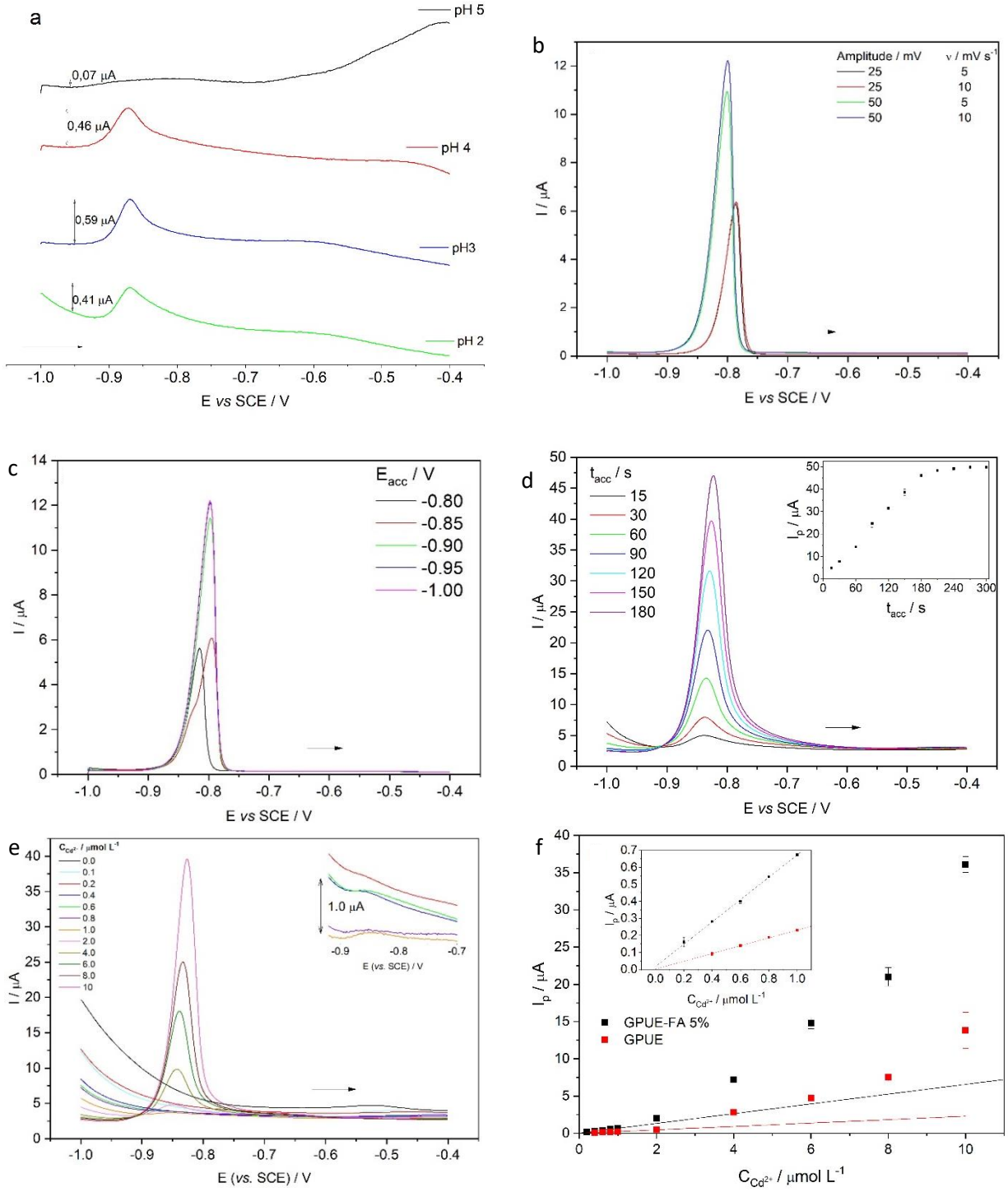

Fig. 5 Differential pulse voltammograms of GPUE-FA 5% for a 1.0 x 10^{-5} mol L^{-1} Cd(II) solution in 0.10 mol L^{-1} KCl (a) by varying the pH (t_{acc} = 1 min, a = 50 mV, v = 10 mV s^{-1}); (b) for various amplitude and scan rates (pH = 3, t_{acc} = 1 min, E_{acc} = -1.0 V (*vs*. SCE)); (c) for various accumulation potentials, E_{acc} (pH = 3, t_{acc} = 1 min, a = 50 mV, v = 10 mV s^{-1}); (d) for various accumulation times, t_{acc} (pH = 3, E_{acc} = -1.0 V (*vs*. SCE), a = 50 mV, v = 10 mV s^{-1}); and the (e) analytical curve obtained for 0.0 to 10.0 µmol L^{-1} Cd(II) solution at GPUE-FA 5% and (f) Analytical curve for the determination of Cd(II) in KCl at GPUE and GPUE-FA 5%, highlighting the linear range(pH = 3, t_{acc} = 3 min, a = 50 mV, v = 10 mV s^{-1}, E_{acc} = -1.0 V (*vs*. SCE))

Barros et al. Fig.

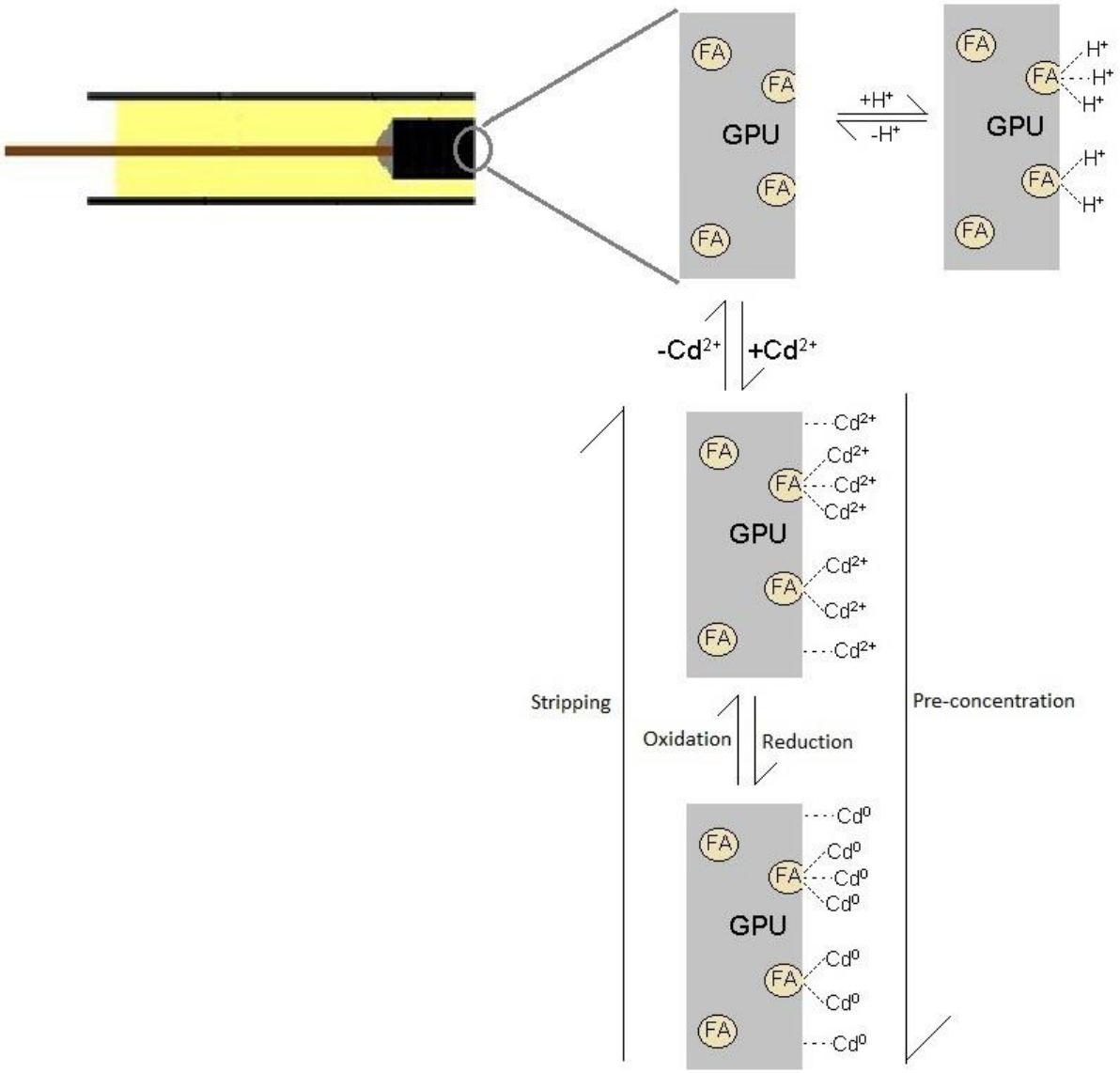

Fig. 6 Schematic representation of the action of FA in the pre-concentration of Cd^{2+} (as a model), on the surface of GPUE-FA 5% (*m/m*).

Development of coal fly ash modified graphite-polyurethane composite electrodes for the determination of Cd(II) in batteries and water

Caio Ribeiro de Barros[1], Priscila Cervini[1], Rafael Martos Buoro[1], Elizabet M. van der Merwe[2] and Éder T. G. Cavalheiro[1*]

Supplementary files

Table S1 Elemental and atomic percentage found at the matrix and modifier regions as determined by EDX

Element	GPU Matrix		FA Modifier	
	Element %	Atomic %	Element %	Atomic %
C	96.1	98.5	ND	ND
O	ND	ND	30.9	44.5
Mg	<0.1	<0.1	1.4	1.3
Al	1.2	0.6	22.2	19.0
Si	1.3	0.6	38.7	31.8
K	0.3	0.1	1.8	1.1
Ca	0.3	0.1	1.3	0.8
Fe	0.6	0.1	3.8	1.6

*ND = not detected

Table S2 TGA/DTG data for the GPU and GPU-FA composites

Sample	Attribution	Temperature interval / ºC	Mass loss / %
GPU	Polymer decomposition	200.4_5 – 484.9	28.4
	Polymer decomposition	484.9 – 660.7	10.4
	Graphite combustion	660.7 – 854.7	60.7
	Residue	900	0.53_4
GPU-FA 2.5%	Polymer decomposition	207.9 – 596.4	35.7
	Polymer decomposition	596.4 – 649.4	6.0_9
	Graphite combustion	649.4 – 896.6	54.7
	Residue	900	3.5_3
	Net Residue*	900	2.9_9
GPU-FA 5%	Polymer decomposition	218.6 – 534.0	25.4_5
	Polymer decomposition	534.0 – 671.1	14.5
	Graphite combustion	671.1 – 895.7	54,7
	Residue	900	5.3_7
	Net Residue*	900	4.8_4
GPU-FA 10%	Polymer decomposition	213.4 – 597.6	30.8
	Polymer decomposition	597.6 – 633.5	4.6_4
	Graphite combustion	633.5 – 885.1	53.4
	Residue	900	10.9
	Net Residue*	900	10.4

*Net Residue: GPU-FA residue measured at 900 ºC – GPU residue at 900 ºC

Table S3 Values of parameters obtained from EIS spectra for GPUE and GPUE-FA 5% (*m/m*)

Simulated parameters	**GPUE**	**GPUE-FA 5%[a]**
R_S / Ω	29.3	79.4
R_1 / Ω	91.8	122
R_2 / Ω	27.1	-
W_1 / 10^{-3} Mho $s^{(1/2)}$	0.819	1.38
W_2 / 10^{-3} Mho $s^{(1/2)}$	0.293	-
G (K_a) / s^{-1}	307.1	-
G (Y_0) / 10^{-3} Mho $s^{(1/2)}$	0.508	-
CPE_1 / 10^{-6} Mho s^N	12.9	134
CPE_2 / 10^{-6} Mho s^N	39.4	5.42
N (CPE_1)	0.869	0.62
N (CPE_2)	0.953	0.95
χ^2 / 10^{-4}	4.64	3.68

[a] 5.0% FA, *m/m*

Table S4 – Concentration of concomitants in water samples as determined by FAAS

Water sample / Concomitant	$C_{concomitant}$ / µmol L^{-1}		
	Artesian Well	**Mineral**	**Tap**
Li^{+}	ND	ND	ND
Na^{+}	148 ± 1	51.5 ± 0.5	83.8 ± 0.2
Ca^{2+}	8.4 ± 0.1	19.220 ± 0.003	6.93 ± 0.04
Mg^{2+}	67.0 ± 0.4	64.8 ± 0.2	35.2 ± 0.1
Fe^{3+}	ND	ND	4.25 ± 0.09
Ni^{2+}	ND	ND	ND
Pb^{2+}	ND	ND	ND
Zn^{2+}	ND	ND	10.16 ± 0.06

*ND = not detected